

# Noncovalent Interactions of $\pi$ Systems with Sulfur - The Atomic Chameleon of Molecular Recognition

William B. Motherwell,<sup>\*[a]</sup> Rafael B. Moreno,<sup>[a]</sup> Ilias Pavlakos,<sup>[a]</sup> Josephine R. T. Arendorf,<sup>[a]</sup> Tanzeel Arif,<sup>[a]</sup> Graham J. Tizzard,<sup>[b]</sup> Simon J. Coles,<sup>[b]</sup> Abil E. Aliev<sup>\*[a]</sup>

**Abstract:** The relative strength of noncovalent interactions between a thioether sulfur atom and various  $\pi$  systems in designed top pan molecular balances was determined by NMR measurements. Compared to its oxygen counterpart, the sulfur atom displays a remarkable ability to interact with almost equal facility over the entire range of  $\pi$  systems studied, with the simple alkene emerging as the most powerful partner. With the exception of the O...heteroarene interaction, all noncovalent interactions of sulfur with  $\pi$  systems are favoured over oxygen.

Noncovalent interactions involving aromatic systems<sup>[1]</sup> such as  $\pi$ - $\pi$  stacking<sup>[2]</sup> or cation- $\pi$  interactions,<sup>[3]</sup> and the ability of an arene to act as a hydrogen-bond acceptor<sup>[4]</sup> are all firmly established as vital control elements in molecular recognition and consequently underpin vast areas of chemistry and molecular biology. More recently, as a consequence of two virtually simultaneous theoretical studies predicting the strength of the related anion- $\pi$  interaction,<sup>[5]</sup> this area has witnessed intense research activity.<sup>[6]</sup> In parallel, following on from the seminal observation of the attractive lone pair... $\pi$  interaction in stabilizing the Z-DNA structure,<sup>[7]</sup> this force is also rapidly gaining recognition as a new area of supramolecular chemistry.<sup>[8]</sup> Detailed quantifiable knowledge of the relative strength of these weak forces is now therefore considered to be essential for the rational design of organocatalysts,<sup>[9]</sup> new drugs and supramolecular materials, as well as the understanding of three-dimensional structure and function in biological systems.

The conformational analysis of designed molecular balances<sup>[10]</sup> with limited degrees of freedom is a particularly powerful tool for probing the strength, distance and angular dependence of such interactions, and also allows for exploration of all important solvation phenomena.<sup>[11]</sup> Whilst an increasing number of studies in recent years have focused on measuring the O... $\pi$  interaction with electron-deficient arenes and heteroarenes<sup>[12]</sup> we were surprised to note that quantifiable comparative information using such balances to probe

noncovalent interactions involving a sulfur atom with  $\pi$  systems has been almost entirely neglected. The vital role played by sulfur in chemical and biological recognition and in drug development is well recognized.<sup>[13]</sup> As summarized in an ongoing series of excellent reviews,<sup>[1]</sup> the investigation of the S...arene interaction is essentially based on extensive database mining of protein crystal structures. In a significant contribution by Dougherty and coworkers<sup>[14]</sup> the strength of a S...arene interaction in the dopamine D2 receptor has been probed by progressive modulation of the electrostatic surface of the arene through fluorination. To the best of our knowledge, in spite of the fact that theoretical chemists continue to be intrigued by the noncovalent interactions of a sulfur atom with  $\pi$  systems,<sup>[15]</sup> no quantitative experimental measurements have been reported for either simple alkenes or heteroarenes. In terms of a comparative study of the relative strengths of S...arene versus O...arene interactions, we have previously noted a significant preference for sulfur over oxygen in measuring the conformational equilibrium of the oxathiolane derivative (**1**) (Figure 1).<sup>[16a]</sup> This bridged bicyclic framework, together with related congeners, has now served as the pivotal element of our top pan molecular balance system for quantifying a wide range of noncovalent functional group interactions with  $\pi$  systems.<sup>[16]</sup>

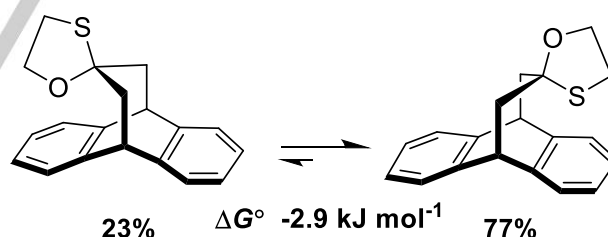


**Figure 1.** S...arene versus O...arene interactions in oxathiolane **1** in CDCl<sub>3</sub> at 298 K.<sup>[16a]</sup>

In a comparison of anisole with thioanisole using a rotameric N-aryl succinimide torsional balance, Cozzi and coworkers<sup>[17]</sup> have reported a marginal preference for an O...arene interaction, but indicated that steric interactions may have contributed. They have also studied the special case of furan versus thiophene using a cyclophane framework.<sup>[12c]</sup> Within these extensively conjugated systems, the more aromatic thiophene was found to adopt a sandwich structure, whilst the furan preferred an O...arene interaction.

In light of the above, there is a clear need for a detailed energy landscape map to provide a comparative data set for both oxygen and sulfur noncovalent interactions over a range of differing  $\pi$  systems. We have accordingly prepared the series of oxathiolanes (**1**) – (**8**), dithioketals (**9**) – (**12**), and ketals (**13**) and

[a] Prof. W. B. Motherwell, Dr. R. B. Moreno, Dr. I. Pavlakos, Josephine R. T. Arendorf, Dr. T. Arif, Dr. A. E. Aliev  
Department of Chemistry  
University College London  
20 Gordon Street, London WC1H 0AJ (UK)  
E-mail: [w.b.motherwell@ucl.ac.uk](mailto:w.b.motherwell@ucl.ac.uk), [a.e.aliev@ucl.ac.uk](mailto:a.e.aliev@ucl.ac.uk)

[b] Dr. G. J. Tizzard, Prof. S. J. Coles  
School of Chemistry  
University of Southampton  
University Road, Southampton, SO17 1BJ

Supporting information for this article is given via a link at the end of the document.

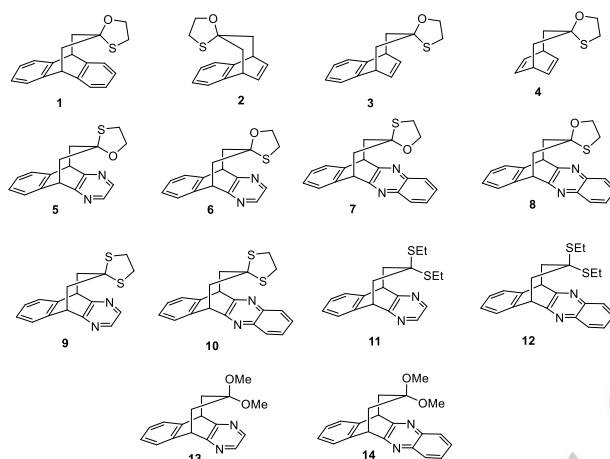


**Figure 2.** Molecular balances (**1**) – (**14**). The structure of the preferred conformer is shown.

(**14**) and measured their conformational preferences in a range of solvents using our previously established NMR methods.<sup>[16]</sup> The results of this study are collected in Table 1 and, even by simple visual inspection of the preferred conformer from a qualitative standpoint, reveal several features of interest.

**Table 1.** Populations of the preferred conformers ( $p$ , in %) in molecular balances (**1**) – (**14**) shown in Figure 2 at 298 K.<sup>[a]</sup>

Solvent	<b>1</b> <sup>[16a]</sup>	<b>2</b>	<b>3</b>	<b>4</b>
CDCl <sub>3</sub>	76.7	86.8	88.2	92.3
C <sub>6</sub> D <sub>6</sub>	64.1	82.3	85.9	
CD <sub>3</sub> CN	70.0	89.6	80.9	
CD <sub>3</sub> OD	69.2	85.1	86.6	
Py- <i>d</i> <sub>5</sub> <sup>[b]</sup>	64.6	81.5	86.5	
DMSO- <i>d</i> <sub>6</sub> <sup>[c]</sup>	72.0	86.4	89.3	
	<b>5</b>	<b>6</b>	<b>7</b>	<b>8</b>
CDCl <sub>3</sub>	77.1	77.5	71.3	83.7
C <sub>6</sub> D <sub>6</sub>	83.4	75.2	68.0	90.5
CD <sub>3</sub> CN	76.7	76.8	72.5	85.8
CD <sub>3</sub> OD	87.0	80.8	79.1	91.0
Py- <i>d</i> <sub>5</sub>	82.9	75.7	70.5	89.0
DMSO- <i>d</i> <sub>6</sub>	77.8	81.5	77.3	82.1
	<b>9</b>	<b>10</b>	<b>11</b>	<b>12</b>
CDCl <sub>3</sub>	64.4	58.6	90.7	94.2
C <sub>6</sub> D <sub>6</sub>	72.0	67.1	90.3	93.7
CD <sub>3</sub> CN	68.8	65.2	90.2	94.0
CD <sub>3</sub> OD	77.1	76.8	93.4	97.1
Py- <i>d</i> <sub>5</sub>	72.8	68.8	90.2	93.6
DMSO- <i>d</i> <sub>6</sub>	72.1	73.8	88.9	95.2
	<b>13</b> <sup>[16d]</sup>	<b>14</b> <sup>[16d]</sup>		
CDCl <sub>3</sub>	90.1	97.0		
C <sub>6</sub> D <sub>6</sub>	91.6	97.0		
CD <sub>3</sub> CN	90.0	97.0		
CD <sub>3</sub> OD	94.3	100.0		
Py- <i>d</i> <sub>5</sub>	90.9	97.1		
DMSO- <i>d</i> <sub>6</sub>	88.4	93.9		

<sup>[a]</sup>Based on the accuracy of NMR  $J$  coupling measurements ( $\pm 0.05$  Hz),<sup>[16c,16d]</sup> the uncertainty in  $p$  values is estimated to be within  $\pm 0.9\%$ . Full details of NMR measurements are provided in Supporting Information. <sup>[b]</sup>Py = pyridine. <sup>[c]</sup>DMSO = dimethyl sulfoxide.

Thus, within the subset of oxathiolanes (**1**) – (**8**) there is a distinct preference in six of these molecules to place the larger sulfur atom (van der Waals radii: O, 1.52 Å; S, 1.80 Å)<sup>[18]</sup> over the  $\pi$  system in preference to the counterbalancing oxygen atom.

Remarkably, this preference is displayed irrespective of whether the noncovalent interaction of the sulfur atom is with an aromatic ring [as in (**1**) and (**2**)], a simple alkene [as in (**3**) and (**4**)], or a heteroarene [as in (**6**) and (**8**)]. For the remaining pyrazine (**5**) and its congeneric quinoxaline derivative (**7**), the noncovalent interaction of the oxygen atom with electron-deficient aromatic heterocycles clearly dominates over the counterbalancing S...arene interaction. The strength of this O...heteroarene interaction (vide infra) can also be seen in the ketals (**13**) and (**14**). Within the series of four dithiolanes (**9**) – (**12**) the S...heteroarene interaction is also preferred over a competing S...arene interaction. This preliminary overview clearly indicates that, whilst the most favoured interaction of an oxygen atom is with the electron-deficient heterocycles, the sulfur atom can interact with an entire range of  $\pi$  systems of differing electronic character. Steric repulsions (defined here in a classical sense, as arising from the fact that a sulfur atom occupies larger space than an oxygen atom) are certainly of little consequence. However, apart from repulsion, there is also a balancing dispersion interaction, which is directly related to polarisability and constitutes the attractive term in the van der Waals equation.<sup>[1b]</sup> Higher polarisability of sulfur compared to oxygen is expected due to the presence of orbitals with higher azimuthal quantum number in S (compared to O), which are likely to diffuse and polarise easier than orbitals with smaller azimuthal quantum number. As sulfur is more polarisable than oxygen, the dispersion interaction is anticipated to be larger for sulfur compared to oxygen. In agreement with this expectation, our results confirm that the sulfur moiety engages more strongly in binding noncovalently in the majority of cases considered in this work.

At a more detailed level, a quantitative comparative estimate of these subtle energy differences can be obtained through consideration of the Gibbs free energy differences ( $\Delta G^\circ$ ) and the derived  $\Delta\Delta G^\circ$  values from pairwise comparison of similar groups of derivatives. Unlike cyclic (**1**) – (**10**), the C–S and C–O bonds are free to rotate in acyclic derivatives (**11**) – (**14**). Furthermore, several additional H...H dispersive interactions between aliphatic hydrogen atoms were revealed from the noncovalent interaction (NCI)<sup>[19]</sup> analysis in (**11**) – (**14**) (see below). We therefore exclude (**11**) – (**14**) from the quantitative estimates and consider only the conformationally constrained cyclic derivatives (**1**) – (**10**). Since errors may either add up or

## COMMUNICATION

cancel out on deriving  $\Delta\Delta G^\circ$  values, we adopt an approach, where a minimum number of  $\Delta\Delta G^\circ$  values are used. In molecular balances (1), (2), (5), (7), (9) and (10), six of eight different pairwise interactions considered in this work are directly compared with the S...arene interaction (see  $\Delta G_1^\circ, \Delta G_2^\circ, \Delta G_3^\circ, \Delta G_4^\circ, \Delta G_5^\circ$  and  $\Delta G_{10}^\circ$  in Table 2). Assuming additivity of free energy contributions, the  $\Delta G^\circ$  value for the remaining S...alkene interaction relative to the S...arene interaction can be estimated using the  $\Delta G_3^\circ - \Delta G_1^\circ$  and  $\Delta G_4^\circ - \Delta G_2^\circ$  differences (Table 2), which provide two independent measurements since they form a chemical double mutant cycle.<sup>[1d]</sup> Thus, it is possible to construct an energy level diagram (Figure 3), which reveals the energies for the set of noncovalent interactions relative to the lowest energy O...heteroarene interaction.

**Table 2.** The Gibbs free energy differences  $\Delta G^\circ$  in (1) – (10) and the derived  $\Delta\Delta G^\circ$  values (in  $\text{kJ mol}^{-1}$ ) from pairwise comparison of similar groups of derivatives in CDC13.<sup>[a]</sup>

Free energy difference	Definition	Value, $\text{kJ mol}^{-1}$
$\Delta G_1^\circ$	$\Delta G_{\text{SAr}} - \Delta G_{\text{OAr}}$	-2.9
$\Delta G_2^\circ$	$\Delta G_{\text{SAr}} - \Delta G_{\text{OEn}}$	-4.7
$\Delta G_3^\circ$	$\Delta G_{\text{SEn}} - \Delta G_{\text{OAr}}$	-5.0
$\Delta G_4^\circ$	$\Delta G_{\text{SEn}} - \Delta G_{\text{OEn}}$	-6.2
$\Delta G_5^\circ$	$\Delta G_{\text{OPz}} - \Delta G_{\text{SAr}}$	-3.0
$\Delta G_6^\circ$	$\Delta G_{\text{SPz}} - \Delta G_{\text{OAr}}$	-3.1
$\Delta G_7^\circ$	$\Delta G_{\text{OQuin}} - \Delta G_{\text{SAr}}$	-2.3
$\Delta G_8^\circ$	$\Delta G_{\text{SQuin}} - \Delta G_{\text{OAr}}$	-4.1
$\Delta G_9^\circ$	$\Delta G_{\text{SPz}} - \Delta G_{\text{SAr}}$	-1.5
$\Delta G_{10}^\circ$	$\Delta G_{\text{SQuin}} - G_{\text{SAr}}$	-0.9
$\Delta G_3^\circ - \Delta G_1^\circ$	$\Delta G_{\text{SEn}} - \Delta G_{\text{SAr}}^{[b]}$	-2.1
$\Delta G_4^\circ - \Delta G_2^\circ$	$\Delta G_{\text{SEn}} - \Delta G_{\text{SAr}}^{[b]}$	-1.5

<sup>[a]</sup> $\Delta\Delta G^\circ = -RT \ln(p/(100-p))$ , in  $\text{kJ mol}^{-1}$ , where  $p$  is the population of the preferred conformer, in %. Abbreviations used: Ar = arene, En = alkene, Pz = pyrazine, Quin = quinoxaline. <sup>[b]</sup>From the two differences shown, the estimated averaged value for  $\Delta G_{\text{SEn}} - \Delta G_{\text{SAr}}$  is  $-1.8 \pm 0.3 \text{ kJ mol}^{-1}$ .

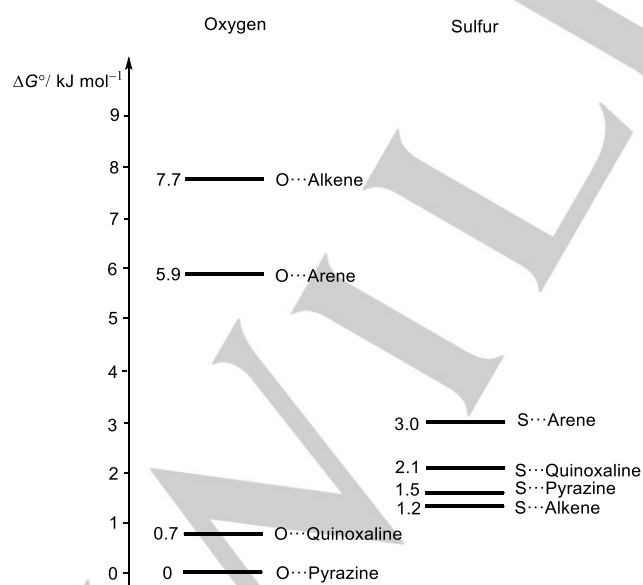


**Figure 3.** Comparative energy level diagram showing the relative energies for noncovalent interactions of  $\pi$  systems with oxygen and sulfur atoms in (1) – (10). All energies shown are relative to that of the strongest noncovalent interaction considered, O...pyrazine in (5).

The main conclusion from this diagram is that, whilst the interactions of the oxygen atom span almost  $8 \text{ kJ mol}^{-1}$ , those involving sulfur are concentrated in a much narrower energy band of  $\sim 2 \text{ kJ mol}^{-1}$ . Even if we consider only the subset of oxathiolanes (1) – (8) and use a larger number of  $\Delta\Delta G^\circ$  values, the estimated energy bands of  $\sim 8$  and  $\sim 2 \text{ kJ mol}^{-1}$  for oxygen and sulfur interactions, respectively, do not change, while values for individual pairwise interactions shown in Figure 3 vary within  $\pm 1 \text{ kJ mol}^{-1}$ . The very small relative energy difference ( $0.6 \text{ kJ mol}^{-1}$ ) between the S...Quinoxaline and S...Pyrazine interactions in favour of the latter was most accurately derived from direct  $\Delta G^\circ$  values for (9) and (10). Density functional theory (DFT) M11-L/def2-TZVP calculations confirm that the corresponding interactions of the oxygen and sulfur atoms span  $8.1 \text{ kJ mol}^{-1}$  and  $3.0 \text{ kJ mol}^{-1}$ , respectively (see below discussion of DFT results and Tables S6 and S7 in Supporting Information). The sulfur atom can, in essence, be described as an “atomic chameleon”, which is capable of blending and participating in noncovalent interactions with almost equal facility irrespective of whether an electron-rich arene or an electron-deficient heteroarene partner is involved. Of equal surprise is the fact that the isolated alkene unit provides the most favourable  $\pi$  interaction for a sulfur atom and the most unfavourable interaction with an oxygen atom. The S...arene and S...pyrazine interactions differ only slightly in favour of the pyrazine, which stands in sharp contrast to the attractive O...pyrazine interaction which is favoured by nearly  $6 \text{ kJ mol}^{-1}$  over the O...arene counterpart. We have previously measured the strength of this O...heteroarene interaction for the hydroxyl group<sup>[16d]</sup> and a similar value has also been reported by Gungl<sup>[12b]</sup> for the noncovalent interaction of an oxygen atom in a 9-benzyl triptycene unit with a highly fluorinated arene. The simplest explanation for the overall pattern displayed by the oxygen atom is that it essentially involves electrostatic interactions, whilst the behaviour of the sulfur atom is dominated by its much greater polarisability (approximately three times larger than that of oxygen)<sup>[20]</sup> and the presence of vacant orbitals for further interaction. As shown previously,<sup>[16a]</sup> in the preferred conformation in (1) (Figure 2), the S...C(Ar) distances are in the range of  $3.2\text{--}4.2 \text{ \AA}$ . The stabilizing effect of S...arene interactions at distances of  $3.5\text{--}4.9 \text{ \AA}$  are known and have been attributed to the availability of empty 3d orbitals on sulfur and its enhanced polarisability.<sup>[1c]</sup> Previously, both experimental and computational techniques have confirmed that inter- and intramolecular dispersion interactions are more important and widespread than assumed in the past.<sup>[1b,21]</sup>

Examination of the results for the ketals (13) and (14) and the dithioketals (11) and (12) are also highly informative. In the first instance, they serve to confirm the measurements made for the oxathiolanes (1) – (8) and dithioketals (9) and (10) in terms of the dominance of the O...heteroarene interaction. The greater number of degrees of conformational freedom in the acyclic ketals allows for the optimal orientation of the oxygen lone pair and the methyl group towards the electron-deficient pyrazine or quinoxaline ring<sup>[16d]</sup> and an even greater measured preference for the O...heteroarene interaction over the O...arene interaction. Similar arguments also apply in the case of the acyclic dithioketals (11) and (12). Intriguingly, the measured conformational populations for the acyclic dithioketals (11) and (12) are virtually identical with their oxygen congeners, whereas the more conformationally restricted 1,3-dithiolanes (9) and (10) display a less marked preference for the sulfur atom to interact with the

## COMMUNICATION

heteroarene as opposed to an arene. This is attributed to the presence of additional H...H interactions between aliphatic H atoms in **(11)** – **(14)**, similar to those found in a methane dimer (see discussion of the NCI results below).

A simple explanation for the main findings from Figure 3 is provided by net atomic charges calculated using a recently described density derived electrostatic and chemical scheme, DDEC6,<sup>[22]</sup> for the three 1,1-dimethyl model systems shown in Figure 4 (see also Tables S3 and S4 in Supporting Information).

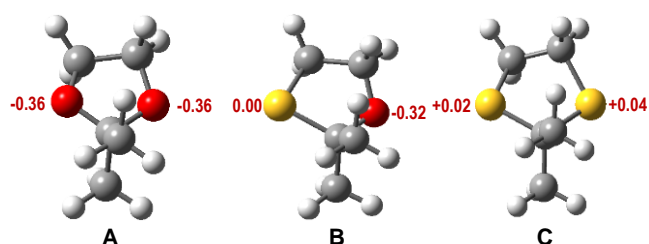


**Figure 4.** Net atomic charges derived from the DDEC6<sup>[22]</sup> analysis of the MP2/aug-cc-pVTZ wave functions. Molecular geometries were optimised in the gas phase at the MP2/aug-cc-pVTZ level of theory.

The net atomic charges show that while the charge on the oxygen atom is significantly negative, the charge on the sulfur atom is essentially 0. Thus, the strongest O...pyrazine interaction is mainly electrostatic in nature, as a negative O atom interacts with the electron-deficient pyrazine ring<sup>[6c,16d]</sup> in **(5)**. At the other end of the oxygen interactions (Figure 3), there are no strong electrostatic interactions for O...Alkene or O...Arene pairs, thus noncovalent interactions of oxygen span over a relatively wide range of  $\sim 8$  kJ mol<sup>-1</sup>. With sulfur, the net atomic charge is  $\sim 0$  and the electrostatic contribution is therefore relatively insignificant regardless of the  $\pi$ -partner. Since dispersive interactions mainly depend on the distance, which does not change significantly in **(1)** – **(10)** [e.g. 3.01 Å in **(5)** and 3.04 Å in **(9)** for the nearest S...C(Ar) pair], we have a narrow band of  $\sim 2$  kJ for sulfur interactions (Figure 3).

In terms of solvation effects, there were no dramatic differences over the range of solvents studied, with the acyclic dithioketals **(11)** and **(12)** and ketals **(13)** and **(14)** being effectively solvent independent. As shown previously,<sup>[11a]</sup> the dispersion interaction energy per unit surface area of contact for two atoms is almost constant and independent of atom type, thus the interactions with third-period atoms are only slightly larger than for the second period, and a small change is expected on replacing oxygen with sulfur. Nevertheless, it was of interest to note that, throughout the entire range of cyclic oxathiolanes and dithiolanes possessing both an aromatic and a heteroaromatic ring, the observed percentage of the already dominant conformer tended to increase with more polar solvents and especially methanol. Curiously, this effect is slightly more marked in those compounds with a sulfur atom exposed to solvent, as in **(5)**, **(7)**, and especially **(9)** and **(10)**, as opposed to an oxygen atom as in **(6)** and **(8)**. Further scrutiny of these subtle solvation effects, especially under various solvent models<sup>[11a,23]</sup> already developed for predicting solute–solvent and individual intramolecular interactions, will certainly be of interest.

The population of the preferred conformer ( $p$ , in %) and the Gibbs free energy differences (in kJ mol<sup>-1</sup>) between the two conformers in molecular balances **(1)** – **(14)** in chloroform were also calculated using various DFT methods (Tables S4 and S5 in Supporting Information). Judging by the value of mean absolute

deviation, the best agreement with the experimental values was found for M11-L<sup>[24a)]/def2-TZVP<sup>[25]</sup> calculations, although the preferred conformer in **(10)** was not correctly identified by this method. The preferred conformers were correctly predicted for all molecular balances **(1)** – **(14)** by M11<sup>[24b)]/def2-TZVP calculations. These findings agree well with the expectation that Minnesota functionals M11 and M11-L are particularly successful for studies of noncovalent interactions.<sup>[24c]</sup> The results of M11-L/def2-TZVP calculations were also used for visualizing noncovalent interactions as real space surfaces by employing the NCI analysis.<sup>[19]</sup> This analysis reveals a colour-coded reduced-density gradient isosurface, in which regions corresponding to attractive interactions are coloured as blue (strong) or green (weak), while repulsive regions are coloured as red (strong) or yellow (weak). The two conformers of **(1)** show green gradient isosurfaces for both noncovalent interactions, with a relatively larger area for the S...arene interaction compared to the O...arene interaction. Similar results were obtained for other molecular balances (Figures S26-S38 in Supporting Information), although in certain cases it was not possible to identify the stronger interaction from the NCI isosurfaces alone (e.g. O...heteroarene vs S...arene in **(5)**, Figure S29). Remarkably, several additional dispersive H...H interactions between aliphatic H atoms were also identified for OMe and SEt groups in **(11)** – **(14)** (Figures S35-S38), similar to that observed between two methane molecules.<sup>[19]</sup></sup></sup>

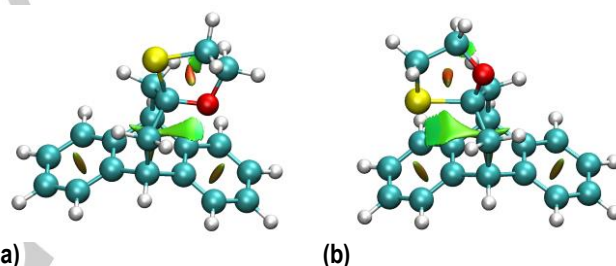


**Figure 5.** NCI surfaces obtained from M11-L/def2-TZVP densities for two conformers of **(1)**, showing the attractive NCI region (in green) between (a) oxygen and the aromatic ring in the minor conformer and (b) sulfur and the aromatic ring in the major conformer.

Throughout our studies,<sup>[16]</sup> single crystal X-ray diffraction has always provided additional insights. In the present instance, six structures, **(2)**, **(5)**, **(6)**, **(9)**, **(10)** and **(14)** have been determined and, in each of these derivatives, the preferred conformer in solution is also observed in the solid state. With the caveat that this is not always the case, it does provide some additional support for the strength of these noncovalent interactions. For the dimethyl ketal **(14)** and the 1,3-oxathiolane **(5)**, both of which feature the O...heteroarene interaction, the distances from the oxygen atom to the centroid of the heteroaromatic ring are 3.113 Å and 3.106 Å, respectively, and lie within the sum of the van der Waals radii (3.22 Å). In similar fashion, for the oxathiolane **(2)**, the oxathiolane diastereoisomer **(6)**, and the two dithiolane derivatives **(9)** and **(10)**, the respective values of 3.236 Å, 3.210 Å, 3.223 Å, and 3.322 Å are all less than 3.50 Å, the sum of the van der Waals radii for sulfur and carbon.

In conclusion, the quantitative data reported above provide clear evidence that, with the exception of the relatively strong O...heteroarene interaction, the thioether sulfur atom is favoured over its oxygen counterpart in noncovalent interactions both with simple alkenes and with arenes. Remarkably, and in stark contrast to the oxygen atom, the sulfur atom can engage, with

## COMMUNICATION

almost equal facility, in its noncovalent interactions with partners ranging from electron rich alkenes and arenes through to electron-deficient heteroarenes. Surprisingly, the strength of the noncovalent interaction between a simple alkene and a sulfur atom is of comparable magnitude to that found for the O...heteroarene interaction.

## Acknowledgements

Support for this work from the Leverhulme Trust is gratefully acknowledged. We also acknowledge equipment support by EPSRC (EP/P020410/1). We wish to thank Dr. Toshiki Nakano (Yamaguchi University, Japan) for preliminary synthetic work and our reviewers for insightful and stimulating comments.

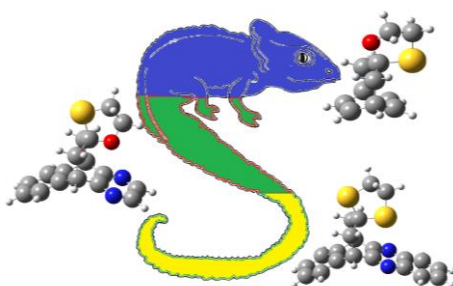
**Keywords:** Conformational analysis • Molecular balances • NMR spectroscopy • Noncovalent interactions • Lone pair •  $\pi$ -interactions

- [1] a) E. Persch, O. Dumele, F. Diederich, *Angew. Chem. Int. Ed.* **2015**, *54*, 3290–3327; *Angew. Chem.* **2015**, *127*, 3341–3382; b) J. P. Wagner, P. R. Schreiner, *Angew. Chem. Int. Ed.* **2015**, *54*, 12274–12296; *Angew. Chem.* **2015**, *127*, 12446–12471; c) E. A. Meyer, R. K. Castellano, F. Diederich, *Angew. Chem. Int. Ed. Engl.* **2003**, *42*, 1210–1250; *Angew. Chem.* **2003**, *115*, 1244–1287; d) S. L. Cockroft, C. A. Hunter, *Chem. Soc. Rev.* **2007**, *36*, 172–199.
- [2] a) C. A. Hunter, J. K. M. Sanders, *J. Am. Chem. Soc.* **1990**, *112*, 5525–5534; b) S. Paliwal, S. Geib, C. S. Wilcox, *J. Am. Chem. Soc.* **1994**, *116*, 4497–4498.
- [3] a) V. P. Santarelli, A. L. Eastwood, D. A. Dougherty, R. Horn, C. A. Ahern, *J. Biol. Chem.* **2007**, *282*, 8044–8051; b) P. Lakshminarasimhan, R. B. Sunoj, J. Chandrasekhar, V. Ramamurthy, *J. Am. Chem. Soc.* **2000**, *122*, 4815–4816; c) D. A. Dougherty, *Acc. Chem. Res.* **2013**, *46*, 885–893.
- [4] a) S. Burley, G. Petsko, *Science* **1985**, *229*, 23–28; b) M. Hirota, K. Sakaibara, H. Suezawa, T. Yuzuri, E. Ankai, M. Nishio, *J. Phys. Org. Chem.* **2000**, *13*, 620–623.
- [5] a) M. Mascal, A. Armstrong, M. D. Bartberger, *J. Am. Chem. Soc.* **2002**, *124*, 6274–6276; b) I. Alkorta, I. Rozas, J. Elguero, *J. Am. Chem. Soc.* **2002**, *124*, 8593–8598.
- [6] a) H. T. Chifotides, K. R. Dunbar, *Acc. Chem. Res.* **2013**, *46*, 894–906; b) S. Matile, A. Vargas Jentzsch, J. Montenegro, A. Fin, *Chem. Soc. Rev.* **2011**, *40*, 2453–2474; c) S. E. Wheeler, J. W. G. Bloom, *Chem. Commun.* **2014**, *50*, 11118–11121.
- [7] M. Egli, R. V. Gessner, *Proc. Natl. Acad. Sci. U.S.A.* **1995**, *92*, 180–184.
- [8] M. Egli, S. Sarkhel, *Acc. Chem. Res.* **2007**, *40*, 197–205.
- [9] A. J. Neel, M. J. Hilton, M. S. Sigman, F. Dean Toste, *Nature* **2017**, *543*, 637–646.
- [10] a) B. Bhayana, C. S. Wilcox, *Angew. Chem. Int. Ed.* **2007**, *46*, 6833–6836; *Angew. Chem.*, **2007**, *119*, 6957–6960; b) L. Yang, C. Adam, G. S. Nichol, S. L. Cockroft, *Nat. Chem.* **2013**, *5*, 1006–1010; c) A. Nijamudheen, D. Jose, A. Shine, A. Datta, *J. Phys. Chem. Lett.* **2012**, *3*, 1493–1496; d) P. Li, C. Zhao, M. D. Smith, K. D. Shimizu, *J. Org. Chem.* **2013**, *78*, 5303–5313; e) H. Gardarsson, W. B. Schweizer, N. Trapp, F. Diederich, *Chem. Eur. J.* **2014**, *20*, 4608–4616.
- [11] a) C. A. Hunter, *Angew. Chem. Int. Ed.* **2004**, *43*, 5310–5324; *Angew. Chem.*, **2004**, *116*, 5424–5439; b) K. B. Muchowska, C. Adam, I. K. Mati, S. L. Cockroft, *J. Am. Chem. Soc.* **2013**, *135*, 9976–9979.
- [12] a) B. W. Gung, X. Xue, H. J. Reich, *J. Org. Chem.* **2005**, *70*, 7232–7237; b) B. W. Gung, Y. Zou, Z. Xu, J. C. Amicangelo, D. G. Irwin, S. Ma, H.-C. Zhou, *J. Org. Chem.* **2008**, *73*, 689–693; c) M. Benaglia, F. Cozzi, M. R. Mancinelli, A. Mazzanti, *Chem. Eur. J.* **2010**, *16*, 7456–7468; d) W. R. Carroll, C. Zhao, M. D. Smith, P. J. Pellechia, K. D. Shimizu, *Org. Lett.* **2011**, *13*, 4320–4323.
- [13] B. R. Beno, K.-S. Yeung, M. D. Bartberger, L. D. Pennington, N. A. Meanwell, *J. Med. Chem.* **2015**, *58*, 4383–4438.
- [14] K. N.-M. Daeffler, H. A. Lester, D. A. Dougherty, *J. Amer. Chem. Soc.* **2012**, *134*, 14890–14896.
- [15] a) C. A. Morgado, J. P. McNamara, I. H. Hillier, N. A. Burton, M. A. Vincent, *J. Chem. Theory Comput.* **2007**, *3*, 1656–1664; b) M. Iwaoka, N. Isozumi, *Molecules* **2012**, *17*, 7266–7283; c) R. Petraglia, C. Corminboeuf, *J. Chem. Theory Comput.* **2013**, *9*, 3020–3025; d) F. Zhou, R. Liu, P. Li, H. Zhang, *New J. Chem.* **2015**, *39*, 1611–1618.
- [16] a) W. B. Motherwell, J. Moïse, A. E. Aliev, M. Nič, S. J. Coles, P. N. Horton, M. B. Hursthouse, G. Chessari, C. A. Hunter, J. G. Vinter, *Angew. Chem. Int. Ed.* **2007**, *46*, 7823–7826; *Angew. Chem.*, **2007**, *119*, 7969–7972; b) A. E. Aliev, J. Moïse, W. B. Motherwell, M. Nic, D. Courtier-Murias, D. A. Tocher, *Phys. Chem. Chem. Phys.* **2009**, *11*, 97–100; c) A. E. Aliev, J. R. T. Arendorf, I. Pavlakos, R. B. Moreno, M. J. Porter, H. S. Rzepa, W. B. Motherwell, *Angew. Chem. Int. Ed.* **2015**, *54*, 551–555; *Angew. Chem.* **2015**, *127*, 561–565; d) I. Pavlakos, T. Arif, A. E. Aliev, W. B. Motherwell, G. J. Tizzard, S. J. Coles, *Angew. Chem. Int. Ed.* **2015**, *54*, 8169–8174; *Angew. Chem.* **2015**, *127*, 8287–8292.
- [17] L. Raimondi, M. Benaglia, F. Cozzi, *Eur. J. Org. Chem.* **2014**, 4993–4998.
- [18] A. Bondi, *J. Phys. Chem.* **1964**, *68*, 441–451.
- [19] a) E. R. Johnson, S. Keinan, P. Mori-Sanchez, J. Contreras-Garcia, A. J. Cohen, W. Yang, *J. Am. Chem. Soc.* **2010**, *132*, 6498–6506; b) J. R. Lane, J. Contreras-Garcia, J.-P. Piquemal, B. J. Miller, H. G. Kjaergaard, *J. Chem. Theory Comput.* **2013**, *9*, 3263–3266.
- [20] (a) M. Swart, J. G. Snijders, P. P. Th. van Duijnen, *J. Comput. Methods Sci. Eng.* **2004**, *4*, 419–425; (b) P. Schwerdtfeger, in *Atoms, Molecules and Clusters in Electric Fields* (Ed.: G. Maroulis), Imperial College Press, London, **2006**, pp. 10–15.
- [21] S. Bartell, *J. Chem. Phys.* **1960**, *32*, 827–831.
- [22] (a) T. A. Manz, N. Gabaldon Limas, *RSC Adv.* **2016**, *6*, 47771–47801; (b) N. Gabaldon Limas, T. A. Manz, *RSC Adv.* **2016**, *6*, 45727–45747.
- [23] (a) C. A. Hunter, *Chem. Sci.* **2013**, *4*, 1687–1700; (b) I. K. Mati, C. Adam, S. L. Cockroft, *Chem. Sci.* **2013**, *4*, 3965–3972.
- [24] (a) R. Peverati, D. G. Truhlar, *J. Phys. Chem. Lett.* **2012**, *3*, 117–124; (b) R. Peverati, D. G. Truhlar, *J. Phys. Chem. Lett.* **2011**, *2*, 2810–2817; (c) R. Peverati, D. G. Truhlar, *Phil. Trans. R. Soc. A* **2014**, *372*, 20120476.
- [25] F. Weigend, *Phys. Chem. Chem. Phys.* **2006**, *8*, 1057–65.

Entry for the Table of Contents (Please choose one layout)

## COMMUNICATION

The relative strength of noncovalent interactions between a thioether sulfur atom and  $\pi$  systems in molecular balances was determined by NMR. The sulfur atom displays a remarkable ability to interact with almost equal facility over the entire range of  $\pi$  systems studied. With the exception of the O $\cdots$ heteroarene interaction, all noncovalent interactions of sulfur with  $\pi$  systems are favoured over oxygen.



*W. B. Motherwell, \* R. B. Moreno, I. Pavlakos, J. R. T. Arendorf, T. Arif, G. J. Tizzard, S. J. Coles, A. E. Aliev\**

**Page No. – Page No.**

**Noncovalent Interactions of  $\pi$  Systems with Sulfur - The Atomic Chameleon of Molecular recognition.**